XXVI. NEUROPHYSIOLOGY

Academic and Research Staff

Prof. Jerome Y. Lettvin
Prof. Stephen G. Waxman
Dr. Isabelle Alter
Dr. Michael H. Brill
Dr. Edward R. Gruberg
Dr. Humberto R. Maturana
Dr. Eric A. Newman
Dr. Donald C. Quick
Dr. Stephen A. Raymond
Dr. Harvey A. Swadlow

Graduate Students

Larry R. Carley
James F. Green
Bradford Howland
Lynette L. Linden
Louis L. Odette
William M. Saidel
Donald W. Schoendorfer

1. THRESHOLD HUNTER DEVICE

Bell Laboratories (Grant)

Louis L. Odette, Stephen A. Raymond

The threshold hunter device places the nerve in a feedback loop so that changes in threshold can be tracked. Where traditional methods for measuring threshold require a series of trial stimuli, to which the responses yield a measure of the response probability for each stimulus level, the threshold hunter forces the stimulus to a level which will produce a response 50% of the time. As this level varies with, for example, temperature or other variables, the hunter follows the variation in accordance with its frequency response. Strictly speaking, the nonlinearity introduced into the feedback loop by the threshold element does not allow determination of the transient response directly from the frequency response, but simulations can be used to choose the "optimal hunting strategy" for a particular situation. The term "optimal hunting strategy" refers to the discrete time filter which is placed in the feedback loop with the threshold element.

2. NERVE MEMBRANE MODELS

National Institutes of Health (Grant 5 ROl EY01149-03S2)
Bell Laboratories (Grant)

Louis L. Odette, Jerome Y. Lettvin

Kinetic reaction sequences for both the sodium and potassium conductance systems have been under investigation. Each sequence involves calcium ion adsorption-desorption on the ion channels, each channel being in one of two conditions, open or closed, depending on the state of the channel sites which bind calcium.

Several types of sequence yield both the steady-state distribution of channel states, in terms of the Hodgkin-Huxley parameters m, n, and h, and the relaxation time

constants, as a function of transmembrane voltage. The models also reproduce the experimental observations of the effects of altered calcium ion concentration on the electrical properties of the axon. With this background, we shall explore the relationship between the models and physical representations of the membrane.

3. RELATION OF THE E-WAVE TO THE DELAYED GANGLION CELL RESPONSE AND THE PROLONGED ROD RESPONSE

National Institutes of Health (Grants 5 TO1 EY00090-04 and 5 RO1 EY01149-03S2)
Bell Laboratories (Grant)

Eric A. Newman, Jerome Y. Lettvin

The e-wave is a delayed component of the electroretinogram which can be recorded from the dark-adapted vertebrate retina. It was first described ten years ago by Crescitelli and Sickel,[1] who recorded e-waves from the isolated retina of the frog. A delayed response can also be recorded from retinal ganglion cells. This activity has been termed the 'delayed ganglion cell response' by Varjú and Pickering.[2]

We have recorded the e-wave and the delayed ganglion cell response simultaneously in order to study the relation between these two delayed responses. A dark-adapted eyecup preparation of the frog (Rana pipiens) was used. The preparation was cooled to 15°C and maintained in a moist 95% O_2-5% CO_2 atmosphere.

Bright flashes (100 ms) of diffuse white light evoked a prominent e-wave which was recorded with an intraretinal electrode referred to the vitreous. The e-wave appeared as a negative notch, or dip (lasting 5 to 15 seconds), superimposed on a slow, positive intraretinal voltage, the slow PIII. Latency to the onset of the e-wave was roughly proportional to the log of stimulus intensity, varying from 2 seconds to over 60 seconds. Simultaneous recordings of ganglion cell activity and the e-wave showed that the two are closely related. Bright stimulus flashes produced a long silent period followed by a prolonged burst of ganglion cell activity which began concurrently with the e-wave. In addition, the length of the delayed ganglion cell response corresponded to the duration of the e-wave response. Bursty ganglion cell activity was associated with an (abnormal) oscillatory e-wave response. These temporal correlations suggest that the two delayed responses represent closely linked retinal phenomena.

The role of the rod receptor response in the generation of delayed retinal responses was investigated. The rod response was recorded differentially between two intraretinal electrodes positioned on either side of the receptor layer in aspartate-treated eyecups. Bright stimulus flashes evoked rod responses consisting of a prolonged (saturated) plateau phase followed by a decay phase. Brighter flashes produced longer delays to the onset of decay. The latency vs log intensity relation of the e-wave response

determined before aspartate treatment was found to match closely the latency vs log intensity relation of the decay phase of the rod receptor response. The onset of the decay phase of the rod response was determined in normal, untreated preparations by measuring the intraretinal b-wave threshold following stimulus flashes. A precipitous drop in the rod phase of retinal threshold, indicating decay of the rod response from a saturated level, always occurred concurrently with the onset of the e-wave.

These experiments demonstrate that the onset of the e-wave (and thus the delayed ganglion cell response) occurs as the plateau phase of the produced rod response begins to decay. This correspondence strongly implies that the latencies at the two delayed responses are determined by the rods.

Preliminary experiments have been conducted in order to localize the origin of the e-wave. Experiments utilizing tetrodotoxin have demonstrated that a normal e-wave can be generated in the absence of ganglion cell spike activity. A source density analysis of the e-wave has shown that the response is primarily generated by a current source near the ganglion cell layer and a current sink near the border between the inner plexiform and inner nuclear layers. This source-sink distribution suggests that the e-wave is mainly generated by proximal elements in the retina.

References

1. F. Crescitelli and E. Sickel, "Delayed Off-Responses Recorded from the Isolated Frog Retina," Vision Res. 8, 801-816 (1968).
2. D. Varjú and S. G. Pickering, "Delayed Responses of Ganglion Cells in the Frog Retina: The Influence of Stimulus Parameters upon the Discharge Pattern," Kybernetik 6, 112-119 (1969).

4. NUCLEUS AND ISTHMI

National Institutes of Health (Grant 5 TO1 EY00090-04)
Bell Laboratories (Grant)

Edward R. Gruberg, Susan B. Udin

In the past year we have completed study of the connections between the nucleus isthmi and the tectum in the frog. These were determined by several anatomical techniques.

The connections between the nucleus isthmi and the tectum in the frog have been determined by several anatomical techniques: iontophoresis of horseradish peroxidase into the tectum, iontophoresis of ^{3}H-proline into the nucleus isthmi and the tectum, and Fink-Heimer degeneration staining after lesions of the nucleus isthmi. The results show that the nucleus isthmi projects bilaterally to the tectal lobes. The ipsilateral

isthmio-tectal fibers are distributed in the superficial layers of the tectum, coincident with the retinotectal terminals. The contralateral isthmio-tectal fibers travel anteriorly adjacent to the lateral optic tract and across the midline in the supraoptic ventral decussation, where they turn dorsally and caudally; upon reaching the tectum, the fibers end in two discrete layers, layers 8 and A of Potter. The tectum projects to the ipsilateral nucleus isthmi, and there is a reciprocal topographic relationship between the two structures. Thus, a retino-tecto-isthmio-tectal route exists which may contribute to the indirect ipsilateral retinotectal projection which is observed electrophysiologically. The connections between the nucleus isthmi and the tectum in the frog are strikingly similar to the connections between the parabigeminal nucleus and the superior colliculus of mammals.

A report of this work has been accepted by the Journal of Comparative Neurology.

This anatomical work has spurred our interest as to what physiological role the nucleus may play. The connections are shown to be both open-loop and closed-loop. We have begun single-unit recording from the nucleus. Preliminary work has revealed that there are at least two types of cells that are akin, to a first approximation, to types 2 and 4 ganglion cell fibers. The units are very susceptible to curare block, and we are developing a preparation which does not need any immobilizing drugs. We have also begun injecting HRP into the nucleus isthmi of a series of animals, and, to our surprise, both superficial and deep tectal cells are stained via retrograde transport.

5. SOMATOSENSORY PROJECTIONS IN THE TECTUM OF THE SALAMANDER IN RELATION TO A MONOAMINERGIC SYSTEM

National Institutes of Health (Grant 5 TO1 EY00090-04)
Bell Laboratories (Grant)

Edward R. Gruberg

After hemisection of the spinal cord or medulla oblongata, a projection has been traced to the inner half of the tectal white of the tiger salamander, using Fink-Heimer degeneration staining. By microelectrode recording it was found that the tectal projection forms a topographic somatosensory map of the contralateral half of the body. This map is in register with the overlying retinotectal visual projection. Using the Falck-Hillarp technique, it was found that the somatosensory tectal input is associated with yellow-fluorescing 5-hydroxytryptamine fibers.

A report of this work has been submitted for publication.

6. ORIGIN OF SPINOTECTAL TRACT

National Institutes of Health (Grant 5 TOl EY00090-04)
Bell Laboratories (Grant)

Edward R. Gruberg

We have recently completed studies on the distribution of the spinal cord cells which project to the salamander tectum. By HRP tectal injection, we have found that most stained spinal cord cells are in a thin, bilateral, mostly medial lamina at the ventral border of the spinal gray. These results very closely match the distribution of fluorescing cells (by the Falck-Hillarp method) which are almost exclusively in this same lamina. We are currently writing a paper containing these results.

7. THRESHOLD OF NERVE MEMBRANE

National Institutes of Health (Grant 5 ROl EY01149-03S2)
Bell Laboratories (Grant)

Stephen A. Raymond, Larry R. Carley

Activity-dependent connectivity among neuronal elements appears to be a basic substrate for information handling. The concept that informational consequences would follow failed invasion of axon branches was first suggested years ago by Walter Pitts, and evidence in accord with that notion has been accumulating since. We have been concerned with activity-dependent variables that will modulate conduction into branches. A major influence is the threshold of the branch, which we have continued to study through the past year. The following are our main observations:

a. Effect of Depression on Refractory Period

Activity rates greater than one impulse every two seconds lead to a progressive increase in threshold called "depression." At higher activities (e.g., 10/s), the depression builds up to an equilibrium level that is 25% -100% greater than resting threshold level. The refractory period of impulses conducted while the nerve is in the depressed phase is extended. The absolute refractory period, during which even the strongest stimuli are ineffective, is prolonged from 2 ms to 3 or 3.5 ms, depending on the severity of the depression. The relative refractory period, during which impulses may conduct but require more intense stimuli than rested nerve requires, is also prolonged. If the depression is strong enough, the threshold never crosses the resting level, indicating that even the maximum period of superexcitability may be above resting threshold following impulses in depressed fibers.

b. Effects of Lithium Ion on Threshold

When 30 mg of LiCl is added to 100 ml of normal Ringer's solution, the resting threshold rises to a level that depends on lithium concentration. This effect was investigated and found to stem from the increased osmolarity of the solution. The effect is a predictable consequence of the change in resistivity of the Ringer's. The observations suggested that alterations in axonal conduction could arise from shifts of osmolarity, but we had been hoping to find a lithium-specific effect. Such an effect was observed on the equilibrium level of activity-induced depression. Even as little as 5 mM LiCl in the Ringer's surrounding an active nerve leads to a gradual reduction of the depression. NaCl and choline chloride result in increased threshold during the depressed phase, probably due to the osmolarity change. These studies form the preliminary observations on which we have designed a plan of study and investigation during 1978, concerning the question of the physiological site and mechanism of the clinical action of lithium ion.

c. Nerve Threshold Chemograph

This device is an extension of the operations involved in tracking thresholds. The activity-dependent threshold curves of axon membrane are used as an index of the effects of neuropharmaceuticals and other chemical agents. In essence, the notion is the same as the case of looking for changes in transistors by watching for shifts in the performance curves. We are seeking to establish a set of operations and procedures that will allow detection and identification of a broad variety of compounds having effects on nerve membrane. Additional experiments are needed, but await the delivery of a programmable threshold hunter. This work will continue into 1978.

8. CONDUCTION VELOCITY VARIATION WITH THRESHOLD

National Institutes of Health (Grant 5 RO1 EY01149-03S2)
Bell Laboratories (Grant)

Stephen A. Raymond

Swadlow and Waxman,[1] S. A. George,[2] and a number of other workers have been studying the aftereffects of impulse activity on conduction velocity. Although a correlation between threshold change and velocity shifts is expected, I studied the extent of this correlation throughout each of the phases of the threshold oscillations following activity. Threshold at the point of stimulation and conduction time over a 6-8 cm distance of axon are well correlated, suggesting that both the changes in threshold and those in conduction velocity may arise in the same processes. Those fibers with largest

threshold variation during activity also showed the largest conduction velocity changes. Changing the concentration of dissolved CO_2 (and hence pH and HCO_3^-) also produced covariation of threshold and conduction velocity.

The strength of the correlation suggests that conduction velocity can be used as an indication of threshold changes in situations where the direct measurement of threshold is difficult. I monitored the conduction velocity during intermittent responsiveness of frog axons exposed to continuous stimulation at levels fixed slightly above threshold. Since stimuli were fixed, my usual means of tracking threshold by changing the duration of each stimulus could not be used. Conduction velocities proved revealing, since at the beginnings of periods of continuous response, they became slower rapidly as the periods of response got longer. Just before failure, the conduction latencies were 20% - 30% longer and the noise in conduction velocity was high. After a period of block, or rest, the next period of responsiveness began with fast conduction velocities. This is in accord with the explanation of intermittent conduction based on threshold changes proposed in 1970. These observations were reported at the Seventh Annual Meeting of the Society for Neurosciences, November 5-10, 1977.[3]

References

1. H. S. Swadlow and S. G. Waxman, "Variations in Conduction Velocity and Excitability Following Single and Multiple Impulses of Visual Callosal Axons in the Rabbit," Exp. Neurol. 53, 115-127 (1976).
2. S. A. George, "Changes in Interspike Interval during Propagation: Quantitative Description," Biol. Cybernetics 26, 209-213 (1977).
3. S. A. Raymond, "Changes in Conduction Velocity Accompany Activity-Dependent Shifts in Threshold of Frog Sciatic Axons," Abstracts for Society for Neuroscience, Vol. III, November 1977, p. 223.

9. DESIGN AND CONSTRUCTION OF AN ARTIFICIAL LARYNX

National Institutes of Health (Grant 5 ROl EY01149-03S2)
Bell Laboratories (Grant)

Donald W. Schoendorfer, Stephen A. Raymond

We have concluded this project this year. A working, internal larynx has been worn successfully by two patients at the Roswell Park Memorial Hospital in Buffalo. Speech restoration was tested using intelligibility tests developed by Professor Kenneth Stevens, of the RLE Speech Communication Group. A natural voice from an unoperated control scored 100, and the M. I. T. Artificial Larynx scored 60. A very commonly used alternative prosthesis, the electrolarynx, scored 4. The spectral quality of the voice is pleasing; it is loud (124 dB vs 127 dB for a normal voice on the same test); dependable,

free from leakage, and acceptable to the small sample of patients so far introduced to it. We are hopeful that the publication of this work will bring the possibility of successful rehabilitation of laryngectomized patients to the attention of surgeons and speech therapists.

10. CYTOCHEMICAL STUDIES ON DIFFERENTIATION OF THE NEURONAL PLASMA MEMBRANE

National Institutes of Health (Grants 5 RO1 NS12307-03, 5 TO1 EY00090-04, and KO4 NS00010)
National Multiple Sclerosis Society (Grant RG-1133-A-1)
Health Sciences Fund (Grant 78-10)

Stephen G. Waxman, Donald C. Quick

A major interest of this laboratory over the past two years has been the differentiation of the neuronal surface in both the normal state and under various pathological conditions. Our previous studies[1, 2] had shown that there are distinct structural differences between the axon membrane at nodes of Ranvier and beneath the myelin in the internodes. Studies on the specialized electrocyte axons in the gymnotic Sternarchus indicated that normally excitable nodes of Ranvier stain intensely on the cytoplasmic surface with ferric ion and ferrocyanide following fixation in cacodylate-buffered aldehydes, while inexcitable nodes along the same axons, despite equal access to the staining solutions, are not stained by this procedure. Comparison of our results with freeze-fracture, pharmacological and physiological data suggested that the ferric ion-ferrocyanide technique might provide a cytochemical marker for regions of the axon membrane with a high sodium-channel density.[3] In order to test this hypothesis, we examined the initial segments of spinal motor neurons following staining with this technique.

On the basis of computer simulation studies on the generation of motor neuron action potentials, Dodge and Cooley[4] predicted that there should be sharp spatial gradients of sodium-channel density over the surface of motor neurons, ranging from low channel density values in the dendrites to high values at the spike initiation region in the initial segment. Their data suggested that in order for the initial segment trigger zone to excite the axon reliably in spite of the electrical load imposed by the soma and dendrites, sodium-channel density at the initial segment should approach that at the node of Ranvier.

Our electron microscopic studies, carried out on rat spinal motor neurons, have demonstrated that following fixation in cacodylate-buffered aldehydes and osmium tetroxide, a subsequent staining with ferric ion and ferrocyanide, aggregates of stain are

localized specifically on the cytoplasmic surface of the initial segment which is deeply stained, in contrast to the cell body and dendrites which do not stain. These results, which provide evidence for a structural differentiation of the neuronal plasma membrane at the initial segment, are consistent with the hypothesis that the ferric ion-ferrocyanide staining procedure may provide a cytochemical marker for regions of high ionic channel density. We are now using this technique to study membrane organization in abnormally myelinated axons (see Sec. XXVI-12) and to study the structure of excitable dendrites.

References

1. D. C. Quick and S. G. Waxman, "Specific Staining of the Axon Membrane at Nodes of Ranvier with Ferric Ion and Ferrocyanide," J. Neurol. Sci. 31, 1-11 (1977).
2. S. G. Waxman and D. C. Quick, "Cytochemical Differentiation of the Axon Membrane in A- and C-Fibers," J. Neurol. Neurosurg. Psychiatry 40, 379-386 (1977).
3. S. G. Waxman, "Conduction in Myelinated, Unmyelinated, and Demyelinated Fibers," Arch. Neurol. 34, 585-590 (1977).
4. F. A. Dodge and J. W. Cooley, "Action Potential of the Motor Neuron," IBM J. Res. Dev. 17, 219-229 (1973).

11. COMPUTER SIMULATION STUDIES ON PREREQUISITES FOR IMPULSE CONDUCTION IN MULTIPLE SCLEROSIS

National Institutes of Health (Grants 5 ROl NS12307-03, 5 TOl EY00090-04, and KO4 NS00010)

Bell Laboratories (Grant)

National Multiple Sclerosis Society (Grant RG-1133-A-1)

Health Sciences Fund (Grant 78-10)

Stephen G. Waxman, Michael H. Brill

Clinical and laboratory observations suggest that it should be possible for action potentials to traverse, in a continuous manner and without interruption, demyelinated zones along some axons. The observation of demyelinated plaques in some asymptomatic patients indicates that at least some demyelinated axons have the capability to conduct impulses. One of the factors which will tend to prevent such conduction is the impedance mismatch at sites of focal demyelination, which may result in a reduction in current density sufficient to cause conduction failure. As part of an effort to examine the pathophysiology and possible modes of symptomatic therapy in multiple sclerosis, we have examined, using computer simulations, the prerequisites, in terms of membrane properties and fiber geometry, for conduction into and beyond a demyelinated region. The present studies of conduction were initiated with a hybrid integration method (implicit internode, explicit node) utilizing a modification of the Crank-Nicholson method of implicit solution of cable equations.[1] Computational parameters and values have been

published previously.[2] Our results are summarized in Figs. XXVI-1 and XXVI-2. As shown in Fig. XXVI-1, at a focally demyelinated fiber with either normal nodal membrane (sodium-channel density = 5000/square micron, based on a conductance of 2.5 pmho/channel) or with Hodgkin-Huxley membrane (500 sodium channels/square micron) in the demyelinated region, presence of sodium channels in the demyelinated region does not insure conduction past this region. Conduction failure may occur at the demyelinated zone, despite normal membrane excitability, as a result of impedance mismatch, i.e., due to insufficient current density. However, as shown in Fig. XXVI-2, our simulations indicate that reduction in length of the two internodes closest to the demyelinated region, to approximately one-third of normal length or less, will facilitate conduction into and beyond the demyelinated plaque. We also examined the prerequisites in terms of channel density necessary to sustain conduction through the plaque

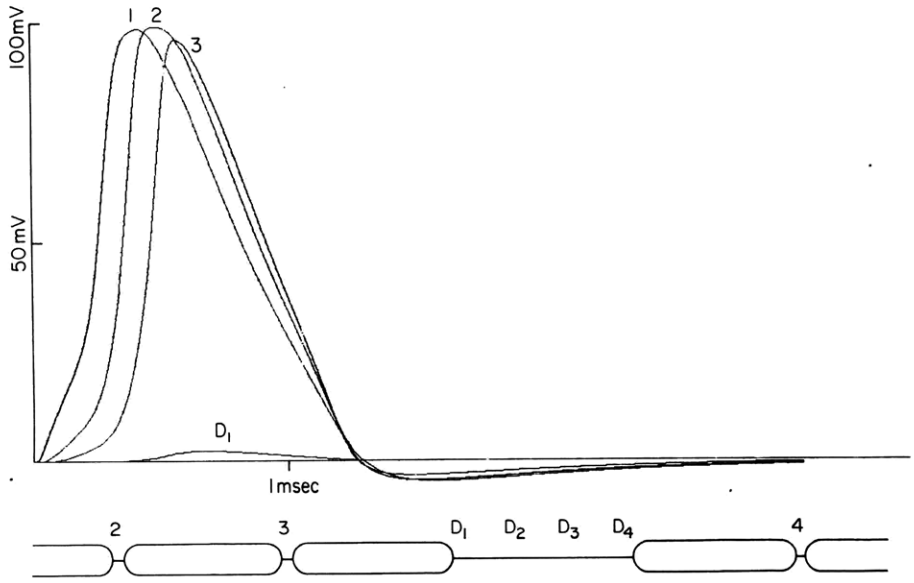

Fig. XXVI-1. Computed action potentials for a fiber focally demyelinated in the region from D_1 to D_4. The axon membrane in the demyelinated region has the same specific membrane properties as normal nodal axolemma. For the fiber shown in this figure, the internode proximal to the demyelinated region ($3\text{-}D_1$) is of normal (2000 μm) length. Despite the assumption of excitable membrane in the demyelinated region, conduction fails at point D_1 as a result of inadequate current density. In this and Fig. XXVI-2, potentials from nodes 1-6 and in the demyelinated region ($D_1\text{-}D_4$) are shown; potentials at nodes 7-11 were computed but are omitted for clarity. Schematic diagrams below the traces show fiber geometry in the vicinity of the demyelinated region; internode 1-2 and all internodes distal to node 4 are of normal length.

and found that a channel density of 200 channels/square micron or greater would suffice to support conduction through the demyelinated region, although again the presence of reduced internode distances proximal to the demyelinated zone was necessary. The present results thus show that reduction in internode distance proximal to a demyelinated region may play a role in permitting action potentials to invade and pass the demyelinated area. In this context it should be noted that histological studies have shown the

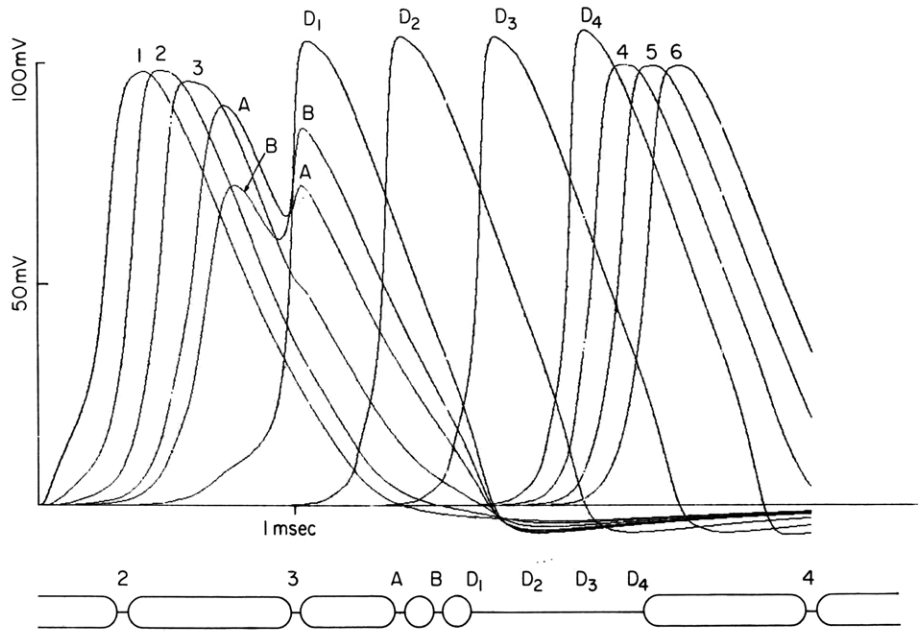

Fig. XXVI-2. Computed action potentials for a fiber similar to that shown in Fig. XXVI-1 with two short internodes (A-B, B-D_1; 400 μm) interposed proximal to the demyelinated region. Under these conditions, the impulse invades the demyelinated region, and passes without interruption into the distal part (e.g., nodes 4, 5, 6) of the fiber.

presence of reduced internode distances along remyelinated fibers. We are led to conclude that, in remyelinated axons, matching of internode distances to functional requirements may be of considerable importance, and that reductions in the internode length may have functional significance in terms of facilitating conduction past focally demyelinated areas.[3]

References

1. J. W. Moore, R. W. Joyner, M. H. Brill, S. G. Waxman, and M. Najar-Joa, "Simulations of Conduction in Uniform Myelinated Fibers: Relative Sensitivity to Nodal and Internodal Parameters," to appear in Biophys. J.

2. M. H. Brill, S. G. Waxman, J. W. Moore, and R. W. Joyner, "Conduction Velocity and Spike Configuration in Myelinated Fibers: Computed Dependence on Internode Distance," J. Neurol. Neurosurg. Psychiatry 40, 769-774 (1977).

3. S. G. Waxman and M. H. Brill, "Conduction through Demyelinated Plaques in Multiple Sclerosis: Facilitation by Short Internodes," manuscript in preparation.

12. ORGANIZATION OF THE AXOLEMMA IN DYSMYELINATED AXONS

National Institutes of Health (Grants 5 ROl NS12307-03 and KO4 NS00010)
National Multiple Sclerosis Society (Grant RG-1133-A-1)
Health Sciences Fund (Grant 78-10)

Stephen G. Waxman, Erika A. Hartwieg
[This work was done in cooperation with Prof. W. G. Bradley, Tufts New England Medical Center.]

As a part of a multidisciplinary study on the demyelinating diseases, we have begun to study the structure of the axon membrane in demyelinated axons (in which there is destruction of myelin) and dysmyelinated axons (in which there is a defect in myelinogenesis). A useful model for the study of dysmyelination is provided by the ReJ dy/dy dystrophic mouse in which many of the spinal root axons exhibit an extreme form of dysmyelination, i.e., amyelination, with the total absence of myelin.[1] In order to study the structural organization of the axon membrane, we have used the cytochemical method described in Sec. XXVI-10, which specifically stains both normal nodal membrane and the membrane at the initial segment, and which we believe may allow visualization of regions of high sodium-channel density membrane.

We examined the lumbar ventral roots of 46-day old, litter mate dy/dy and +/? female mice, following fixation in cacodylate-buffered aldehydes and staining with ferric ion and ferrocyanide as described previously.[2] In both normal roots (from +/? mice) and at the occasional normally myelinated fibers in dystrophic (dy/dy) roots, dense precipitates of stain were present on the cytoplasmic surface of the nodal axolemma. In contrast to this, the amyelinated axons exhibited no dense staining. In some cases a fuzzy undercoating was present subjacent to the axolemma, as has been described following conventional staining at normal nodes of Ranvier. Observations of heminodes, at the junction between myelinated and amyelinated regions, showed thin extensions of the paranodal Schwann cell cytoplasm, in some cases extending for several microns over the initial portion of the amyelinated axon.

The present data show clear structural differences between the axon membrane of the amyelinated axons in dystrophic mice and the axon membrane at normal nodes of Ranvier (as judged by staining with ferric ion and ferrocyanide in both normal and

dystrophic animals). On the basis of results we are tempted to speculate that sodium-channel density may be substantially lower in the amyelinated axon membrane than at normal nodes of Ranvier. It is interesting, in this regard, that Rasminsky et al.[3] have demonstrated continuous conduction along the dysmyelinated parts of some spinal root axons in dystrophic mice. As noted in Sec. XXVI-13, we have examined, using computer simulations, the prerequisites in terms of membrane properties and fiber geometry for such continuous conduction.

References

1. W. G. Bradley and M. Jenkinson, "Abnormalities of Peripheral Nerves in Murine Muscular Dystrophy," J. Neurol. Sci. 17, 227-247 (1973).
2. S. G. Waxman and D. C. Quick, "Cytochemical Differentiation of the Axon Membrane in A- and C-Fibers," J. Neurol. Neurosurg. Psychiatry 40, 379-386 (1977).
3. M. Rasminsky, R. E. Kearney, A. J. Aguayo, and G. M. Bray, "Conduction of Nervous Impulses in Spinal Roots and Peripheral Nerves of Dystrophic Mice," to appear in Brain Res.

13. NEUROPHYSIOLOGY OF CONDUCTION ALONG AXONS IN THE NORMAL CNS

National Institutes of Health (Grants 5 RO1 NS12307-03 and KO4 NS00010)
National Multiple Sclerosis Society (Grant RG-1133-A-1)
Health Sciences Fund (Grant 78-10)

Harvey A. Swadlow, Stephen G. Waxman

Our previous studies on conduction along axons in the corpus callosum of the rabbit indicated that conduction properties of these axons are not invariant in the temporal domain, but, on the contrary, vary with the history of previous impulse activity along the axon. In particular, the conduction properties of each axon are determined by the sequence: action potential → refractory period → supernormal period → subnormal period. (This is described elsewhere in greater detail.[1]) During the past year we have addressed two additional problems: impulse conduction along axons within the primate brain; and development of a modified criterion of latency invariability for the identification of antidromically activated neurons.

a. Impulse Conduction along Axons within the Primate Brain

For these studies, extracellular recordings were obtained from single neurons in the prelunate gyrus of the Rhesus monkey, Macaca mulatta. These studies utilized methods similar to those which we have described previously.[2] Impulse conduction along callosal axons was studied by measuring latency to antidromic activation of cell

bodies following constant current stimulation via chronically implanted electrodes. Stimulating electrodes were placed intracortically in the contralateral prelunate gyrus and also under visual control into the posterior portion of the corpus callosum. Antidromically activated neurons were identified by collision techniques. For neurons which were shown to be antidromically activated, latency to a test stimulus was determined at various intervals following a single suprathreshold conditioning delivered through the same stimulating electrode or following a spontaneous impulse. As had previously been found in callosal axons in the rabbit, variations in both threshold and latency of the response to a test stimulus occur following a single conditioning stimulus. Threshold was therefore determined at each conditioning stimulus/test stimulus interval, and intensity of the test stimulus was always adjusted to 1.2 × this threshold value.

Each of more than 40 neurons tested showed a period of supernormal impulse conduction following the relative refractory period of a single prior impulse. Peak magnitude of the decrease in latency occurred at intervals of 4-12 ms and was generally from 5% to 10% of controlling antidromic latency. Duration of the supernormal period ranged from 30 ms to more than 150 ms. If a train of conditioning pulses was presented instead of a single conditioning pulse, a subnormal period of decreased conduction velocity and excitability was observed to follow the initial increase in conduction velocity and excitability. Duration and magnitude of the subnormal period were both dependent upon the number and duration of the conditioning pulses. Many neurons were shown to take several seconds to return to control levels after a conditioning train of 10 or 20 pulses. Some callosal axons could be antidromically activated from both midline callosal and contralateral cortical stimulation sites. For such axons the magnitude of the variations in antidromic conduction latency was approximately proportional to the control latency at each stimulation site. These results indicate that variations in antidromic latency reflect variations in the conduction velocity distributed along the axon under study. The results of the present study, as in those of previous studies, indicate that variations in conduction velocity and excitability to the test stimulus are a function of prior activity in the axon under study rather than the result of ephaptic interactions between axons or some other artifact of prior electrical stimulation. Thus, variations in latency occur following spontaneous as well as electrically elicited prior impulses.

In addition, control experiments showed that while no decrease in latency occurred to a test stimulus that followed a conditioning stimulus which is just subthreshold, decreases in latency of similar magnitude and time course occur to a test stimulus that follows a conditioning stimulus presented at either 1.1 or 2.0 × threshold. Finally, additional control procedures have shown that when the intensity of a conditioning stimulus is just at threshold, a decrease in latency to the test stimulus only occurs when the initial conditioning stimulus results in a spike.

The present results extend our observations on activity-dependent variations in

conduction velocity and excitability to axons within the brain of the primate. Similar observations have been made within the past year by Kocsis et al.[3] in the axons of caudate nucleus neurons, and Renaud and Hopkins[4] in the axons of hypothalamic neurons. The results of Raymond and Lettvin[5] address the question of the mechanisms underlying these aftereffects of activity.

In the rhesus monkey, where interhemispheric conduction distances are less than 60 mm, we have observed variations in interhemispheric conduction time of more than 6 milliseconds. In the human, where interhemispheric distances may exceed 100 mm, we would anticipate variations in axonal conduction time of an even greater magnitude. Such variations in conduction time may significantly affect the temporal summation and coding of neural information.

References

1. S. G. Waxman and H. A. Swadlow, "Conduction Properties of Axons in Central White Matter," Prog. in Neurobiol. 8, 297-324 (1977).
2. H. A. Swadlow and S. G. Waxman, "Variations in Conduction Velocity and Excitability Following Single and Multiple Impulses of Visual Callosal Axons in the Rabbit," J. Exp. Neurol. 53, 128-150 (1976).
3. J. D. Kocsis, C. P. Vander Maelen, and S. T. Kitai, "Conduction Properties of Caudate Afferent Axons in the Cat," Abstracts for Society for Neuroscience, Vol. III, November 1977, p. 40.
4. L. P. Renaud and D. A. Hopkins, "Amygdala Afferents from Mediobasal Hypothalamus," Brain Res. 121, 201-213 (1977).
5. S. A. Raymond and J. Y. Lettvin, "Aftereffects of Activity in Peripheral Axons as a Clue to Nervous Coding," in S. G. Waxman (Ed.), Physiology and Pathobiology of Axons (Raven Press, N. Y.; in press).

14. NEUROPHYSIOLOGY OF DEMYELINATED CENTRAL AXONS IN SITU

National Institutes of Health (Grants 5 RO1 NS12307-03 and KO4 NS00010)
National Multiple Sclerosis Society (Grant RG-1133-A-1)
Health Sciences Fund (Grant 78-10)

Stephen G. Waxman, Jeffery D. Kocsis

We are beginning a series of studies on the neurophysiology of impulse conduction along demyelinated axons within the mammalian brain. The studies will utilize our previous data on impulse conduction along normal central axons within rabbit corpus callosum for normative data.[1] We now intend to study impulse conduction in this same system following the production of focal demyelinating lesions. We are at present investigating various methods for producing such lesions. We intend to produce focal lesions

in such a manner that it will be possible to study impulse conduction along demyelinated and normally myelinated regions of the same fiber, so that each fiber will act as its own control. We then intend to compare the physiology of conduction in demyelinated and normally myelinated regions of these fibers and to study their pharmacology. As in our previous studies on impulse conduction in the CNS, we are doing correlative ultrastructure and cytochemistry on the affected axons. Our ultimate goal in this research is the development of appropriate models with which to screen pharmacological agents of possible use in multiple sclerosis.

References

1. S. G. Waxman and H. A. Swadlow, "Conduction Properties of Axons in Central White Matter," Prog. Neurobiol. 8, 297-324 (1977).

15. NOVEL FORM OF LETTER CHART FOR EYE TESTING

National Institutes of Health (Grant 5 TO1 EY00090-04)
Bell Laboratories (Grant)

Bradford Howland

The familiar Snellen eye-testing chart uses large, black, serifed letters on a white background, and is the universal standard by which visual resolution is compared. A disadvantage of the Snellen chart is the fact that defocused letters can still be partially recognized by their blur patterns; much time is thus wasted as the patient attempts to guess the letter. The layout of this chart is further complicated by the fact that each letter has a different degree of recognizability.

Analysis of the spatial frequency content of the Snellen letters reveals that they contain high and low spatial frequencies in generous measure. We have recently experimented with charts in which the low spatial frequency components have been filtered out, or are absent by design.

Figure XXVI-3 shows such a chart, using superimposed transfer letters of the same type font. The basic letter stroke is a black line with a white stripe down the middle and is placed on a neutral gray background having the same average luminosity as the stripe. When viewed from a distance, the letters of the new chart behave as follows: (a) When the letters are too small to be recognized, they disappear from view, rather than being unrecognizable blurs. (b) The distance at which disappearance occurs is determined by width of the letter stroke, and each of the letters has very nearly the same visibility. Thus, the choice of letters, or the particular choice of type font is largely immaterial to the design of the new chart, as long as the stroke of the letter is uniform in width.

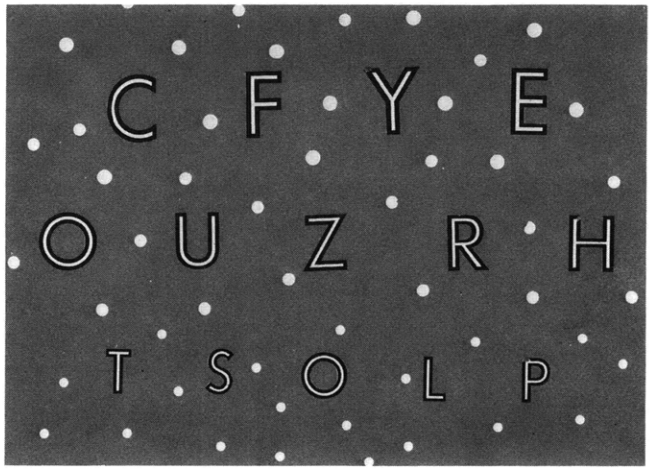

Fig. XXVI-3. Photograph of new letter chart with superimposed array of dots. Letters were formed by superimposed black (futura inline) and white (futura demi-bold) transfer lettering (chartpak) on a 25% reflecting neutral gray surface. (The shade of gray in this offset print may differ appreciably.)

For these effects to occur, the photometric balance of the letter-stroke versus the gray background must be accurate to a few percent, and the shade of gray must be chromatically neutral since defocused letters against a warm (brownish) gray appear as blue outlines. The requirement of accurate photometric balance effectively rules out hand-drafting of the letters; we have therefore made use of available transfer letters, in outline, and solid forms of the same type font.

Achievement of photometric balance in the symmetrical triphasic letter-stroke goes a long way toward minimizing the low spatial frequency content of the letter. The ideal lowpass filtered letter stroke would be a thin white line (a delta function) with a gray surround, modulated by the sin x/x function. Since such a letter stroke is impractical at present, we are investigating the Fourier transform functions for three- and five-element solid black and white strokes of various proportions.

More recently, we have added to the new letter chart a galaxy of randomly placed stars, dots, or asterisks having a diameter equal to the stroke width, with approximately three to five stars per letter. This refinement greatly inhibits the recognition of letters of marginal visibility. This is evidently due to the fact that the solid white or black stars which have appreciable low-spatial-frequency content retain their visibility, when defocused, more than do the letters, thus functioning as an effective "noise" background. When, however, the letters are in focus, the background of stars is easily ignored. With the addition of the stars or dots photographic reproductions of the charts, which were unsatisfactory because of uneven gray scale, functioned as well as the originals.

An obvious extension of the method is to use a set of outline drawings of simple

objects, in which each picture would have a different stripe width on the same gray background. These could be used for the testing of very young children and other illiterates.

We wish to thank Dr. Jerome Rosner, formerly at the New England College of Optometry, for helpful discussions and suggestions.

16. NEW TYPE OF SUBJECTIVE PUPILLOMETER

National Institutes of Health (Grant 5 TO1 EY00090-04)
Bell Laboratories (Grant)

Bradford Howland

We have constructed an instrument that permits a subject to measure the diameter of his/her pupil to an accuracy of approximately 0.2 mm in light or dark-adapted condition. The optical design of this instrument, which utilizes a strong, crossed-cylinder lens, is such that it does not exhibit the large errors, due to uncertain refraction or subject accommodation, of previously described instruments, such as the entoptic pupillometer of Allen, described by I. M. Borish.[1] The instrument presents a set of four circular blur patterns with sharp outlines: the subject turns a knob that adjusts the spacing until the patterns are tangent. The instrument is simple to operate but is subject to the usual uncertainties, due to the ease with which pupil diameter varies with subjective and psychological factors. The instrument uses light-emitting diodes and a simple mechanism, and could perhaps prove useful in the monitoring of therapy with drugs such as the tricyclid antidepressants, that noticeably affect pupil size.

References

1. Clinical Refraction (The Professional Press, Inc., Chicago, 3rd ed., 1970), p. 249.

17. ELECTRONIC ABERRATION SYNTHESIZER

National Institutes of Health (Grant 5 TO1 EY00090-04)
Bell Laboratories (Grant)

Bradford Howland

The electronic aberration synthesizer is a device with which a subject can determine the first nine coefficients in the polynomial describing the aberrations of the lens of his eye. The subject adjusts the controls of the aberration generator, until the elements of a perceived grid pattern are linear and parallel. The apparatus has been built,

calibrated, and tested, using the designer as subject, and tests with a group of subjects will shortly commence. An aim of our study will be to test whether the statistical averages of aberration coefficients obtained with an entirely subjective method, using analysis of the drawings of 55 subjects, are repeatable with the new method.[1] Furthermore, we hope to determine correlations of the new aberration data with the subject's performance on letter-test charts, of traditional and newer designs.

References

1. H. C. Howland and B. Howland, "A Subjective Method for the Measurement of Monochromatic Aberrations of the Eye," J. Opt. Soc. Am. 67, 1508-1518 (1977).

18. A FIGURE SHOWING BLUE-BLACK REVERSAL WITH INCREASED VIEWING DISTANCE

National Institutes of Health (Grant 5 TO1 EY00090-04)

Michael Brill, Bradford Howland

In our efforts to understand the special role of the blue receptor in color vision, we constructed a display of blue and black felt marker lines on white construction paper partly painted with yellow tempera, such that the blue and black appearances reversed when viewing distance was increased.

A reduced facsimile of the display is shown in Fig. XXVI-4. The entire figure was originally 12 inches high. The black lines (width 1/16 inch) were separated from the yellow areas by 1/4 inch of white. The dark blue line (width 1/8 inch) was between the two yellow areas (width 1 inch).

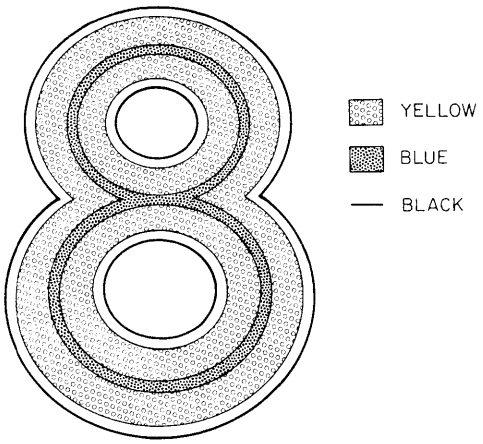

Fig. XXVI-4. Blue-black reversal with increased viewing distance.

When viewed under incandescent light from a distance of 3 feet, the blue and black lines were readily identified in accordance with the pigment names. From 10-15 feet, however, most observers saw the black lines change to blue and the blue line to black.

The change of blue to black can be attributed to the rather low spatial resolution of the blue-sensitive visual mechanism compared to that responsible for assessing contrasts of brightness. Hence the blue and the adjacent complementary yellow cancel as seen by the blue mechanism, leaving a sensation of no hue at the site of the dark line.

The change of black to blue is more difficult to explain by such conventional arguments. It is not easy to understand why the complementary blue induced at the edge of each yellow field (partly by eye movements across the boundary into the white region) is ascribed to the black line by the perceiver.

19. BINOCULAR AFTERIMAGE EFFECT

National Institutes of Health (Grant 5 TO1 EY00090-04)

Michael Brill

We have recently observed a striking binocular afterimage effect: Illuminating one eye can cause the polarity of an afterimage already present in the other eye to change (transiently) from negative to positive.

One can easily observe the effect as follows:

Look briefly with the left eye at an intense green light, and then look with the same eye at a piece of white paper under incandescent light. The long negative (dark) afterimage occasioned by the green light will look magenta at first and then turn bluish-purple. This happens whether or not the right eye is open. Closing the left eye or dimming the light on the white paper makes the afterimage turn bright green (positive).

Now repeat the procedure, but introduce a steady, intense light into the right eye as you look at the white paper with the left eye. Irrespective of the color of the light in the right eye, the afterimage in the left eye will flash bright green for a second and then return to a dark purple appearance. The effect is most pronounced when the light in the right eye is spatially uniform (i. e., a Ganzfeld), for then there can be no binocular rivalry with the afterimage. A Ganzfeld of appropriate intensity can also be made by illuminating the right eye through a ping pong ball with a 500-watt projector from 3 feet away.

As long as the negative afterimage persists, the green flash can be elicited repeatedly by turning the Ganzfeld light on and off. In general, the flash is the same color as the light occasioning the afterimage (i. e., the flash is a positive homochromatic afterimage).

The green (homochromatic) flash cannot be attributed to stray light entering the left

eye from the illuminant producing Ganzfeld on the right eye: More light in the left eye just makes the afterimage appear darker and more purple. On the contrary, the flash effect is similar to the polarity reversal that happens when light is dimmed in the left eye.

One can demonstrate that the green flash is the result of dimming of the light in the left eye caused by sympathetic iris contraction in the left eye from the Ganzfeld in the right eye. Repeat the above experiment, but replace the white piece of paper with a moderate white light in Maxwellian view. This can be done by interposing a lens between the eye and a distant light source, such that the near focal point of the lens is in the plane of the pupil and at its center. When all the light passes through the center of the pupil, it will not be affected by iris contraction. Now look at an intense Ganzfeld light with the right eye, and the green flash will not appear.

The time course of the green flash may be the combined effect of the transience of the pupil reflex and the adaptation of receptors to the dimmed light. It is interesting to note that the perceptual effect of the afterimage reversal is far greater than that of the general dimming of the visual field caused by the sympathetic iris contraction.

20. DEVICE FOR ILLUMINANT-INVARIANT ASSESSMENT OF CHROMATIC RELATIONS

National Institutes of Health (Grant 5 TO1 EY00090-04)

Michael Brill

For a large class of illuminant spectra and object spectral reflectances, we have designed a trichromatic photosensing device that compares the light reflected from several objects in its visual field, and computes quantities characteristic of the compared reflectance spectra of these objects, independent of the illuminant spectrum. Although the design makes no direct suggestions for human color vision, such an invariance could be helpful in color constancy.

The design[1] follows the approach of H. Yilmaz.[2] Over a visible wavelength range $\phi \in [0, 2\pi]$, define three photoreceptor spectral sensitivities

$$q_1(\phi) = 1, \qquad q_2(\phi) = 1 + \sin(\phi), \qquad q_3(\phi) = 1 + \cos(\phi).$$

Suppose the energy spectrum of the illuminant is uniform in space and time, and varies slowly enough in wavelength so that it is adequately represented by the first three terms in its Fourier expansion in ϕ. Then, for some a_1, a_2, a_3, the illuminant spectrum $I(\phi)$ is given by

$$I(\phi) = a_1 + a_2 \sin(\phi) + a_3 \cos(\phi).$$

Let each (nonfluorescent) reflecting object i have a reflectance spectrum constrained only by the stipulation that it has no Fourier components in $\cos(2\phi)$ or $\sin(2\phi)$. (We exclude these components in order to insure the invariance that follows.) Then the reflectance spectrum $r_i(\phi)$ for the i^{th} object is

$$r_i(\phi) = b_{i1} + b_{i2} \sin(\phi) + b_{i3} \cos(\phi) + \sum_{k=3}^{\infty} [c_{ik} \cos(k\phi) + d_{ik} \sin(k\phi)].$$

Note that we have allowed a tremendous freedom in the possible spectra of reflectance, which can be very jagged. Chlorophyll is one example of a natural pigment with this property.

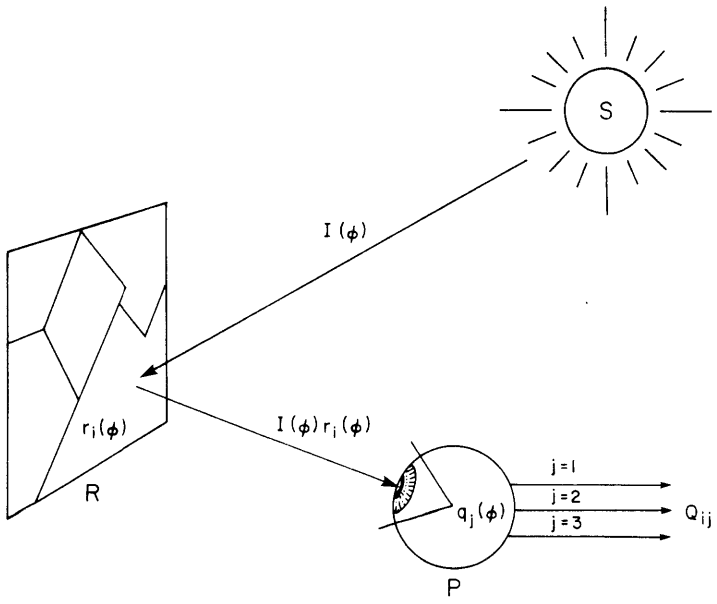

Fig. XXVI-5. Reception of reflected light by the photosensor.

If a triad of photoreceptors, each with a different spectral sensitivity, receives light from object i, three linear filtrates (tristimulus values) Q_{ij} are obtained (see Fig. XXVI-5), given by the integrated products of the illuminant spectrum, the i^{th} reflectance spectrum, and the spectral sensitivity of the j^{th} photopigment ($j = 1, 2, 3$):

$$Q_{ij} = \int_0^{2\pi} r_i(\phi)\, I(\phi)\, q_j(\phi)\, d\phi.$$

From these assumptions, it follows that the tristimulus vector (Q_{i1}, Q_{i2}, Q_{i3}) of an object i is an invertible linear transformation of the object color 3-vector (b_{i1}, b_{i2}, b_{i3}), with the coefficients depending only on the illuminant parameters a_j. Thus a ratio of

tristimulus volumes is independent of illuminant, and is an assessable measure of relationships among the object spectral reflectances. Implications for experiments such as those of Land[3] are discussed elsewhere.[1]

The design may be generalized as follows: over a visible wavelength region $\lambda \in [\lambda_1, \lambda_2]$, define n^{th} degree polynomials $P_n(\lambda)$ $(n = 0, 1, 2, \ldots)$ orthogonal with respect to a weighting function $w(\lambda)$. For $j = 0, 1, 2$, define $q_j(\lambda) = P_j(\lambda)\, w(\lambda)$. Over the visible range, approximate the illuminant spectrum by

$$I(\lambda) = \sum_{k=0}^{2} a_k P_k(\lambda)$$

and the reflectances by

$$r_i(\lambda) = \sum_{\ell=0,\, \ell \neq 3,4}^{\infty} b_{i\ell} P_\ell(\lambda).$$

Then once more the illuminant incurs a linear transformation on the object color 3-vectors (b_{i1}, b_{i2}, b_{i3}) to make the tristimulus vectors (Q_{i1}, Q_{i2}, Q_{i3}), and hence tristimulus volume ratios are once again illuminant-invariant.

It should be noted that when an illuminant change shows up as an invertible linear transformation on object tristimulus vectors, the inverse of the transformation can be constructed if three of these vectors are known before and after the change. Thus, under the above assumptions, a device with prior information about three object colors can reconstruct all the others in its visual field, thereby attaining invariance in the appearance of each individual object as well as in their relationships.

References

1. M. H. Brill, "A Device Performing Illuminant-Invariant Assessment of Chromatic Relations," accepted for publication in J. Theor. Biology.

2. H. Yilmaz, "On Color Vision and a New Approach to General Perception," in E. E. Bernard and M. R. Kare (Eds.), Biological Prototypes and Synthetic Systems, Vol. 1 (Plenum Press, New York, 1962), p. 126.

3. E. Land, "Color Vision and the Natural Image. Part 1," Proc. Nat. Acad. Sci. 45, 115 (1959).